Green Chemistry

Accepted Manuscript

Green Chemistry

Cutting-edge research for a greener sustainable future

www.rsc.org/greenchem

Volume 1 | Number 1 | Jan 2013 | Pages 1–100

Stille couplings in water @RT

ROYAL SOCIETY OF CHEMISTRY

ROYAL SOCIETY OF CHEMISTRY

www.rsc.org/greenchem

Journal Name

ARTICLE

Enantioselective aerobic oxidation of olefins by magnetite nanoparticles at room temperature: a chiral carboxylic acid strategy

Leila Hadian-Dehkordi[a] and Hassan Hosseini-Monfared[*,a]

Asymmetric oxidations of organic compounds are limited in their synthetic scope and by practical factors, such as the use of complex catalyst synthesis. A simple and cheap nanostructured catalyst system comprising magnetite nanoparticles stabilized by L-(+)-tartaric acid (Fe_3O_4/tart-NPs) were successfully synthesized in diethylene glycol. The catalyst was characterized by FT-IR, TGA, ICP-AES, XRPD, SEM and dynamic light scattering (DLS). Catalytic activity of Fe_3O_4/tart-NPs dispersion in acetonitrile in the presence of isobutyralhyde was studied in selective aerobic oxidation of olefins to form asymmetric epoxide, an important intermediate for the synthesis of biologically active compounds. In addition, the magnetically recoverable nanocatalyst Fe_3O_4/tart-NPs can be conveniently separated and recovered from the reaction system by applying an external magnetic field and reused for five cycles without the loss of activity after each cycle. These results demonstrate that the heterogeneous nanocatalysts possess potential applications for green and sustainable development. As synthesized nanoparticles of Fe_3O_4/tart-NPs are a chip and easy to synthesize asymmetric catalyst which were prepared without involvement of difficult and cumbersome procedure for the synthesis of complicated asymmetric ligands. Possible reaction mechanisms were outlined.

Introduction

Chiral compounds are commonly required in the pharma, agrochemical, and fine chemical sectors.[1] In the synthesis of chiral compounds, chiral epoxides are one of the most valuable and versatile building blocks.[2] Epoxides containing one or two stereogenic centers are reactive precursor that can be readily involved in further asymmetric transformations through, for example, asymmetric ring-opening reactions.[3] Ever since the pioneering work of the Sharpless epoxidation of allylic alcohols and the Katsuki-Jacobsen epoxidation of unfunctionalized olefins, there has been great progress in asymmetric epoxidation over the past decades.[4,5]

Given the far lower cost, less toxic and greater abundance of iron over the more precious metals, it is clear that iron derived catalysts would provide a range of benefits if they could be made practical, stable, active and selective. In recent years, significant breakthroughs have been made in the development and applications of homogeneous iron-based

catalysts to asymmetric transformations.[6] There are difficulties, however, in adapting this type of process for commercial purposes. The soluble catalysts suffer from problems associated with the separation, recovery, and instability at high temperatures. On the other hand, catalytic methods which are used routinely in bulk chemical manufacture, employing heterogeneous catalysts are not generally applicable for the production of chiral products.[7] The unique combination of magnetic nanoparticles and catalytically active species presents the opportunity to solve a range of catalyst recovery problems.[8] Organocatalysts supported by magnetic nanoparticles act under favourable quasi-homogeneous conditions and can be recycled by simple magnetic decantation rather than time-consuming and energy-intensive filtration or centrifugation.[9] Magnetically recoverable nanocatalysts have been used in organic synthesis for a wide range of catalytic reactions.[10,11] Ikenberry and co-workers achieved monolayer sulfonic acid-functionalized iron oxide nanoparticles as solid acid catalyst for carbohydrate hydrolysis.[12] Magnetite nanoparticle-supported asymmetric catalysts based on 4,4'-disubstituted BINAP-Ru-DPEN complexes were used for enantioselective hydrogenation of aromatic ketones (BINAP = 2,2'-bis(diphenylphosphino)-1,1'-binaphthyl; DPEN = diphenylethylenediamine).[13] Gawande et al. summarized reported studies on nano-magnetite (Fe_3O_4) as

[a.]Department of Chemistry, University of Zanjan 45195-313, Zanjan, Islamic Republic of Iran.

COMMUNICATION

Journal Name

a support for the immobilization of homogeneous metals, organocatalysts, ligands, N-heterocyclic carbenes and their applications.[14] Zhao et al. studied organic superbase-functionalized magnetic Fe_3O_4 as catalyst for the fixation of CO_2 with 2-aminobenzonitriles, resulting in the synthesis of quinazoline-2,4(1H,3H)-diones.[15] Katsuki and Egami reported iron-catalyzed asymmetric aerobic coupling of 2-naphthols.[16] Subramanian et al. achieved magnetite catalysts incorporated with M (Cu, Ni, Zn, and Co) promoters for high temperature water gas shift reaction.[17] Cano and co-workers performed cross-alkylation of primary alcohols with an impregnated iridium on magnetite catalyst.[18] Godoi et al. applied Fe_3O_4 nanoparticles for the synthesis of alkynyl chalcogenides from terminal acetylenes and diorganyl dichalcogenides.[19]

Asymmetric oxidation using ubiquitous molecular oxygen as the oxidant and the "free" nanoparticles of abundant iron as the catalyst has attracted a growing interest.[20] Previously, we have reported the synthesis and catalytic activity of magnetite nanoparticles (Fe_3O_4-NPs) in diethylene glycol in the presence of carboxylic acids.[21] Carboxylic acid plays a critical role in determining the morphology, particle size and/or size distribution and catalytic activity of the resulting particles. The resulting nanoparticles can be easily dispersed in aqueous media and other polar solvents due to coated by a layer of hydrophilic polyol and carboxylic acid ligands in situ. Easily prepared Fe_3O_4/carboxylic acid-NPs showed recyclable and highly selective catalytic activity for the epoxidation of cyclic olefins with aqueous 30% H_2O_2.[21] On the other hand, there are some reports on the effects of carboxylic acid and chiral ester on asymmetric oxidation. For example, chiral bipyrrolidine based iron and manganese complexes catalyze the asymmetric epoxidation of various olefins with H_2O_2 in the presence of carboxylic acid additives with high efficiency and selectivity, and with good to high enantioselectivity.[22] The most widely used protocol for the asymmetric epoxidations of acyclic E-enones bearing two alkyl substituents uses TBHP in the presence of a sub-stoichiometric quantity of a magnesium tartrate catalyst.[23] Furthermore, one of the most successful ways of inducing enantioselectivity in a heterogeneous catalytic system is by the adsorption of chiral "modifier" molecules on the reactive metal surface.[24]

Considering the above observations and our previous work motivated us to study the catalytic performances of L-(+)-tartaric acid stabilized nano-magnetite (Fe_3O_4/tart-NPs) as a recyclable and green asymmetric oxidation catalyst under aerobic and mild reaction conditions. Among various oxidants, molecular oxygen is a cheap, clean and readily available oxidant.[25,26] Isobutyraldehyde was used as reductant for the reduction of diogygen at the beginning of the reaction and it is co-oxidized with substrate. This type of co-oxidation was first studied by Mukaiyama and co-workers.[27] This system (Fe_3O_4/tart-NPs) represents the first example of asymmetric induction from magnetite stabilized by asymmetric tartaric acid, as well as a rare example of catalytic enantioselective olefin epoxidation by magnetite nanaoparticles (MNPs) and dioxygen.[28,29,30] Unprotected MNPs are often unstable and tend to aggregate during the catalytic transformations,

resulting in a remarkable drop of the catalytic capability due to the decrease of MNPs surface areas.[31]

Experimental

Materials and instrumentation

L-(+)-Tartaric acid ((2R,3R)-(+)-tartaric acid, >99%, Merck), iron(III) chloride hexahydrate ($FeCl_3 \cdot 6H_2O$, 98% Fluka), diethylene glycol (99%, Merck), cyclohexene (99%, Fluka), 1-methyl-1-cyclohexene (97%, Sigma-Aldrich), alpha-methyl styrene (>99%, Merck), cis-stilbene (>95%, Merck), $trans$-stilbene (96%, Sigma), 1,2,3,4-tetrahydronaphthalin (>98%, Merck), thioanisole (>99%, Merck) and other reagents were obtained from commercial sources and were used as received without further purification.

The reaction products of the oxidation were determined and analyzed by HP Agilent 6890 gas chromatograph equipped with an HP-5 capillary column (phenyl methyl siloxane 30 m × 320 μm × 0.25 μm) with flame-ionization detector. The enantiomeric excess (ee%) was determined by chiral GC (HP 6890-GC) using a SGE-CYDEX-B capillary column (25 m × 0.22 mm ID× 0.25 μm). ^1H NMR spectra of reaction mixture (without purification) were recorded on a Bruker 250 MHz spectrometer. UV–Vis spectra of solution were recorded on a Shimadzu 160 spectrometer. Fourier transform infrared (FT-IR) spectra were recorded using a Perkin-Elmer 597 spectrophotometer after making pellets with KBr powder. Powder X-ray diffraction patterns were collected at the Bruker, D8ADVANCE, Germany, wavelength 1.5406 Å (Cu Kα), voltage: 40 kV, current, 40 mA. The size and morphology of solid compounds were recorded by using a Hitachi F4160 scanning electron microscope (SEM) operated at an accelerating voltage of 10 KV. The hydrodynamic diameter of the nanoparticles was measured using the Zetasizer Nano-ZS3600 (Malvern Instruments, Malvern, UK) dynamic light scattering (DLS) with the sonicated nanoparticles in water before measurement. Magnetization measurement was performed at room temperature using a vibrating sample magnetometer (VSM) device, in the Development Center of the University of Kashan (Kashan, Iran). Textural properties determined from N_2 adsorption isotherms measured on a Belsorp mini II (Japan) instrument.

Synthesis of Fe_3O_4/tart-NPs

Magnetite nanoparticles stabilized with chiral tartaric acid (Fe_3O_4/tart-NPs) was synthesized according to our previously reported procedure.[21] In a typical experiment, $FeCl_3 \cdot 6H_2O$ (0.81 g, 3 mmol), L-(+)-tartaric acid (0.075 g, 0.5 mmol) and urea (1.80 g, 30 mmol) were completely dissolved in diethylene glycol (30 mL) by vigorous mechanical stirring. The obtained yellow clear solution was sealed in a Teflon lined stainless steel autoclave (23 mL capacity) and then heated at 200 °C for 4 h. After cooling down to room temperature, the black magnetite were separated magnetically and washed with ethanol for several times to eliminate organic and inorganic impurities, and then dried at 60 °C for 6 h (Scheme 1).

Fe$_3$O$_4$-NPs were synthesized similarly without using L-tartaric acid.

Catalytic aerobic oxidation of cyclohexene with Fe$_3$O$_4$/tart-NPs

The oxidation reactions were carried out in a glass inlay of a 32 mL steel autoclave. The autoclave was conditioned by evacuation and re-filling with dioxygen. All autoclave loading was carried out under air. In a typical experiment, 2.0 mmol of substrate was added to the reactor with 0.001 g Fe$_3$O$_4$/tart-NPs, 5.0 mmol isobutyraldehyde and 0.1 g chlorobenzene as an internal standard. After purging with O$_2$, the reactor was pressurized to 2 bar. Stirring rate was 375 rpm. At the end of 7 h the reactor was depressurized, the catalyst removed by an external magnet (1.2 T) and the product mixture was analyzed by ^{1}H-NMR and gas chromatography. Conversions and yields were calculated with respect to the starting substrate. The products were identified with authentic samples and ^{1}H- and ^{13}C-NMR spectroscopic data. The reaction products were quantified by gas chromatography and identified by comparison with the retention time and spectral data to those of an authentic sample. To ensure reproducibility each catalytic reaction was carried out at least two or three times.

For recycling experiments, after completion of the reaction, the nanocatalyst was recovered using a magnet, washed with acetonitrile, dried and reused without further purification. GC condition with column Hp-5: carrier gas N$_2$ flow = 0.7 mL/min, inlet temp 250 °C, initial column temp 90 °C, final column temp 190 °C, sleep 10 °C /min. GC condition with column Cydex-B: carrier gas N$_2$ flow = 0.7 mL/min, inlet temp 200 °C, initial column temp 50 °C, final column temp 150 °C, sleep 10 °C /min.

Proof of stereochemistry

Prochiral olefins, tetralin and thioanisole were oxidized by Fe$_3$O$_4$/tart-NPs and isobutyraldehyde/O$_2$. Analysis of the corresponding chiral products by chiral GC was used to determine the enantioselectivity of the reaction. The absolute configuration was established by comparing the GC data with those observed for R-(+)-limonene.

Results and discussion

The crystalline nature of the as-synthesized L-(+)-tartaric acid protected iron oxide nanoparticles was determined by wide angle X-ray powder diffraction (XRD). Fig. 1 shows the XRD patterns of Fe$_3$O$_4$ and Fe$_3$O$_4$/tart nanocrystals. The Intensity of the peaks decrease by functionalization of Fe$_3$O$_4$. In the case of Fe$_3$O$_4$/tart-NPs, using intense peak at 2theta = 35.423, FWH = 0.590, we get crystallite size of 14.1 nm by X'Pert program. Six characteristic peaks (2θ = 30.3°, 35.4°, 43.2°, 53.5°, 57.2° and 62.9°) corresponding to (220), (311), (400), (422), (511) and (440) planes of cubic inverse spinel Fe$_3$O$_4$ are obtained.[32] The positions and relative intensities of all diffraction peaks for both Fe$_3$O$_4$-NPs and Fe$_3$O$_4$/tart-NPs match well with those expected for Fe$_3$O$_4$ rather than for γ-Fe$_2$O$_3$. XRD is relatively insensitive to the difference between magnetite (Fe$_3$O$_4$) and

maghemite (γ-Fe$_2$O$_3$), and the Raman and IR spectra have been proved to be an alternative tools.[33,34]
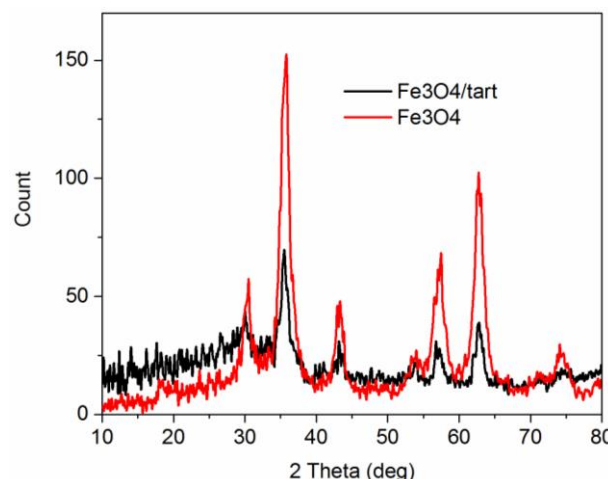
Fig. 1 XRD patterns of the synthesized Fe$_3$O$_4$-NPs and Fe$_3$O$_4$/tart-NPs.

The FT-IR spectra of the tart, Fe$_3$O$_4$-NPs and Fe$_3$O$_4$/tart-NPs nanoparticles are shown in Fig. 2. The L-tartaric acid spectrum shows a dominant peak at 1732 cm^{-1}, resulting from the carbonyl stretch ν(C=O) associated with protonated carboxyl groups,[35] which was reduced in intensity with adsorption/chemisorption of tartaric acid on Fe$_3$O$_4$ as the carboxyl groups deprotonated in Fe$_3$O$_4$/tart nanoparticles. As the intensity of the carbonyl peak waned at Fe$_3$O$_4$/tart, peaks at 1550 cm^{-1} and 1422 cm^{-1} appeared. These two features represent the asymmetric ν$_{as}$(CO$_2^-$) and symmetric ν$_s$(CO$_2^-$) carbon–oxygen stretches of carboxylate groups respectively.[36,37] These results revealed that L-tartaric acid was chemisorbed onto the Fe$_3$O$_4$-NPs as a carboxylate.[38]

The presence of both the ν(C=O) vibrations of the acid COOH functionality at 1732 cm^{-1} and the ν$_s$(CO$_2^-$) vibration of the carboxylate group at 1422 cm^{-1}, reveal that the L-tartaric acid is adsorbed as a monotartrate species which is bound to the surface via the deprotonated carboxylate group. In addition, the free and intact COOH acid group is held away from the surface and the lack of downshift in frequency of the ν(C=O) vibration of this group suggests that it is not involved in intermolecular H-bonding interactions with the alcohol groups of neighbouring monotartrate species, which is in contrast to the adsorption of L-tartaric acid on a Cu(1 1 0) surface at 300 K.[24,39] IR bands can be used to distinguish the type of the interaction between the carboxylate group and the metal atom. Carboxylate groups which are chelating or coordinating with each O atom to a metal atom exhibit differences between the asymmetric and symmetric stretching frequencies, which are less than the ionic value (Δν = 164 cm^{-1} for the acetate ion).[36] For Fe$_3$O$_4$/tart-NPs Δν = 1550–1422 = 128 cm^{-1} suggests a chelate action of each tartaric acid carboxylate group toward the iron oxide nanoparticles, as shown in Scheme 1.

Fig. 2a and Fig. 2c clearly show the characteristic lattice vibration of magnetite at 576 cm^{-1} and 420 cm^{-1}.[40] These results are consistent with the as-synthesized nanocrystals being Fe$_3$O$_4$ rather than γ-Fe$_2$O$_3$. In the Fe–O range, synthetic

COMMUNICATION

Journal Name

maghemite shows broad IR bands at 668, 630, 442 cm^{-1}.[40] The broad characteristic band at 3441 cm^{-1} could be assigned to O-H stretching vibration arising from the Fe–OH groups on nanoparticles, the carboxylic groups of tartaric acid, and adsorbed water.[41] In addition, for Fe$_3$O$_4$-NPs and Fe$_3$O$_4$/tart-NPs the dominant H-O-H bending vibration of water is seen at 1632 cm^{-1}.[42]
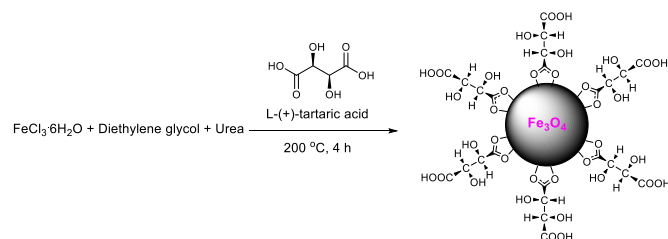
Scheme 1 Preparation of Fe$_3$O$_4$/tart nanoparticles

The thermal stability of Fe$_3$O$_4$/tart-NPs was examined by means of TGA, and the result is shown in Fig. S1 (in Supporting information). It is seen that the sample exhibits continuous weight loss of ~17% from 25 to 141 °C due to the removing of adsorbed H$_2$O and the O-H functional groups from the surface of magnetite. The weight loss of 6% in the temperature range of 141-362 °C should be mainly due to the decomposition of the supporting tartaric acid and the content of Fe$_3$O$_4$ is 77%. The weight loss of ~6% of the sample is observed above 141 °C, indicating the existence of enough supporting ligand. The supporting tartaric acid (C$_4$H$_6$O$_6$) functional groups might play an important role in stabilizing magnetite nanoparticles, promoting the magnetite catalytic activity and inducing chirality in the oxidation products (vide infra). The content of Fe$_3$O$_4$ in Fe$_3$O$_4$/tart-NPs sample was confirmed with measuring iron of the sample by ICP technique (51% iron).
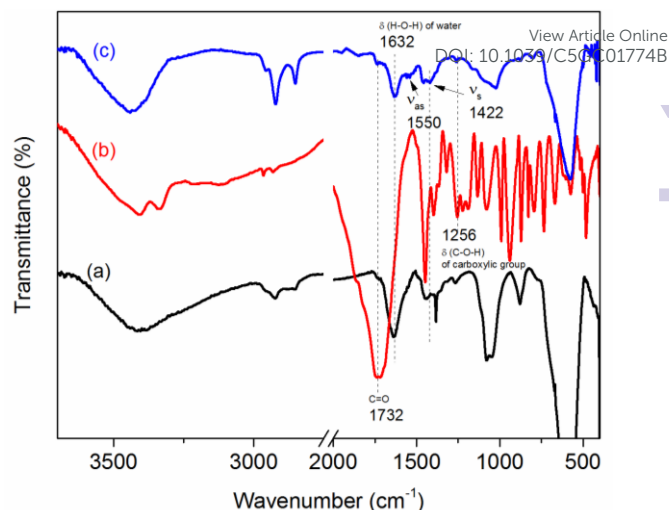
Fig. 2 FT-IR spectra of (a) Fe$_3$O$_4$-NPs, (b) L-(+)-tartaric acid (tart) and (c) Fe$_3$O$_4$/tart-NPs.

The size, shape and size distribution of the nanoparticles of Fe$_3$O$_4$/tart-NPs were examined by SEM (Fig. 3). SEM image show that the magnetite particles obtained in the presence of L-(+)-tartaric acid have nearly spherical shape and uniform size distribution with an average size of 19.5 ± 4.2 nm. The synthesized Fe$_3$O$_4$-NPs without using L-tartaric acid show the particles with average size of 373 ± 88 nm (Fig. 3c). By using the carboxylic acid the resulting nanoparticles became more uniform and the average diameter decreased dramatically. Carboxylic acid affects the morphology, particle size and size distribution of the magnetite particles.[21] The nanoparticles of Fe$_3$O$_4$/tart-NPs are stable and preserve their shape and uniform distribution after catalysis (vide infra). After four times recycle in the catalytic oxidation of cyclohexene, the nanoparticles are well separated and their size increased to 239.3 ± 66.3 nm (Fig. 3; b).

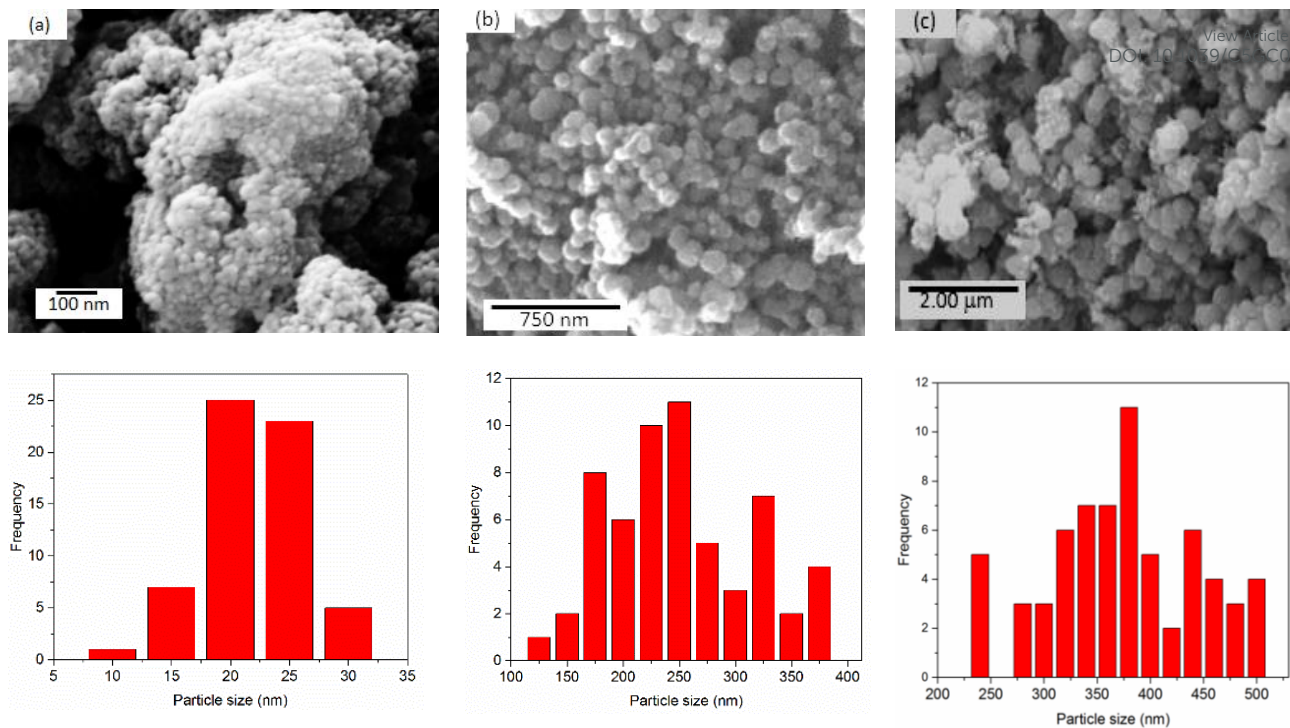**COMMUNICATION**

Fig. 3 SEM images and particle size distribution of (a) Fe_3O_4/tart-NPs as-synthesized, (b) recovered Fe_3O_4/tart-NPs after use (see the next section) and (c) Fe_3O_4-Nps.
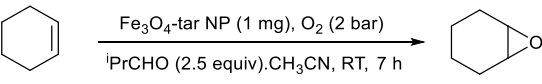
Journal Name

ARTICLE

Dried powder of the present sample was easily redispersed in neutral water solution and its hydrodynamic size was determined by dynamic light scattering (DLS) to be 74 nm (Fig. S2) and demonstrate the monodispersity of the nanoparticles. Usually, the particles size in solution is approximately three times of their values in the solid state because of hydration. According to DLVO theory,[43] NPs are stabilized by a combination of van der Waals interactions and double-layer forces. In the system described herein, van der Waals interactions presumably originate from the carboxylic group providing electrostatic stabilization.

Analysis of the magnetic properties of the synthesized Fe_3O_4/tart-NPs indicated a superparamagnetic nature of the material (Fig. S3). The magnetization value of Fe_3O_4/tart-NPs is approximately the same with the value of Fe_3O_4-NPs and higher than the magnetization of core-shell Fe_3O_4/SiO_2-NPs.[44] This finding shows the negligible effect of diamagnetic tartaric acid coating over the Fe_3O_4-NPs and a favorable property for magnetic separation by a conventional magnet.

Catalytic oxidation

Having synthesized and characterized the Fe_3O_4/tart nanocomposite, its role as a heterogeneous catalyst was then evaluated for the oxidation of olefins. We first examined the reaction using magnetite nanoparticles as a catalyst in air oxidation of cyclohexene at 25 °C (Table 1). Cyclohexene is more prone to both epoxidation and allylic oxidation[45] and oxygenation of cyclohexene is a good probe to provide evidence for or against a non-radical mechanism and to evaluate the catalyst selectivity. While isobutyraldehyde, tart/isobutyraldehyde or Fe_3O_4-NPs without tartaric acid showed poor oxidation catalysis (Table 1, entries 1-3) and using the mixture of $FeCl_3 \cdot 6H_2O$ + L-tartaric acid gave no epoxide (entry 4), only Fe_3O_4/tart-NPs bearing tartaric acid as stabilizer exhibited oxidation catalysis (entry 7). Presence of co-oxidant isobutyraldehyde is essential for activation of dioxygen and acetonitrile as solvent provide better medium than methanol (entries 5 and 6). In fact, the catalyst does not work in methanol (entry 6), however its activity in acetonitrile is remarkable. The possibility of involvement of acetonitrile as co-reactant, through peroxyimidic acid as an oxygen donor, was excluded in the oxidation reactions, since no $MeCONH_2$ under the catalytic oxidations was detected.[46] The polarity of acetonitrile (dielectric constant $\varepsilon/\varepsilon_0$ = 37.5 where ε_0 is the electric permittivity of free space) is higher than methanol (32.7).[47] Probably, the polarity, low coordinating ability and aprotic nature of acetonitrile play the main roles in improving the activity of the catalyst in acetonitrile.

The ground state of molecular oxygen is a triplet with two unpaired electrons having parallel spins. Therefore, the direct reaction of molecular oxygen with a singlet organic molecules is a spin-forbidden process.[48] With regard to aerobic oxidation catalyzed by transition-metal complexes, several reactions involving the combined use of molecular oxygen with reducing agents such as $NaBH_4$, 2-propanol and aldehyde have been studied.[49,50] Co-oxidation of cyclohexene and isobutyraldehyde under the investigated conditions leads to the formation of cyclohexene oxide (main product) and isobutyric acid. The oxidation of cyclohexene was not occurred by using a substochiometric amount of isobutyraldehyde (isobutyraldehyde/substrate ratio = 0.2, 0.5), Table 1, entry 8. In order to be sure that the oxidation of the substrates proceeds up to its maximum extent, a large stoichiometric excess of isobutyraldehyde with respect to the substrate (2.5 times of substrate) was used.

Table 1 optimization of carboxylic acid mediated olefin oxidation

Fe₃O₄-tar NP (1 mg), O₂ (2 bar)

ⁱPrCHO (2.5 equiv).CH₃CN, RT, 7 h

Entry	Catalyst	Reductant	Solvent	Conv. (%)[b]	Epoxide selectivity (%)[b]
1	none	ⁱPrCHO	CH_3CN	0	0
2	tart	ⁱPrCHO	CH_3CN	0	0
3	Fe₃O₄-NPs (no tart)	ⁱPrCHO	CH_3CN	3.2	99
4	FeCl₃·6H₂O + tart [c]	ⁱPrCHO	CH_3CN	56	0 [d]
5	Fe₃O₄/tart-NPs	None	CH_3CN	0	0
6	Fe₃O₄/tart-NPs	ⁱPrCHO	CH_3OH	0	0
7	Fe₃O₄/tart-NPs	ⁱPrCHO	CH_3CN	58±4[e]	61±7 [e]
8	Fe₃O₄/tart-NPs	ⁱPrCHO [f]	CH_3CN	0	0

[a] Reaction conditions: Fe₃O₄/tart-NPs 1.0 mg, isobutyraldehyde (ⁱPrCHO) 5 mmol, cyclohexene 2 mmol, solvent 3 ml, chlorobenzene (internal standard) 0.1 g, O₂ 2 bar, room temperature, reaction time 7 h. [b] As compared to chlorobenzene as an internal standard. Conversion and selectivity were determined by GC and is an average of at least two runs. [c] FeCl₃·6H₂O 0.12 mmol, tart 0.02 mmol; the ratio of tart/Fe is equal to the ratio used for Fe₃O₄/tart-NPs synthesis. [d] the other products were cyclohex-2-en-1-ol 49 % and cyclohex-2-en-1-one 7 %. [e] Average of 6 runs; the other products were cyclohex-2-en-1-ol 38 ± 8 % and cyclohex-2-en-1-one 1%. [f] isobutyraldehyde 1 mmol.

Under the optimized conditions, aerobic oxidation of various olefins was studied (Table 2). Increasing the reaction time up to 13 h gave almost the same results. Thereby, the minimum reaction time which results to the highest conversion and yield was chosen. Tetralin and thioanisole were also examined to explore the scope of the catalytic activity of Fe₃O₄/tart-NPs. Highest enantioselectivity (99%) and epoxide selectivity (100%) were obtained in the oxidations of 1-decene with 77% conversion and 1-octene with 48% conversion (Table 2, entries 1 and 2). The epoxide selectivity for 1-methyl-1-cyclohexene was also 100%, however enantioselectivity decreased to 62% (entry 3). The oxidation of styrene, alpha- and beta-methylstyrene were occurred by breaking the double bond and mainly benzaldehde and acetophenone obtained (entries 4, 5 and 7). Probably, the stability of the plausible intermediate benzyl radical favours breaking of the olefin double bond. In spite of the lower epoxide selectivity in the oxidation of alpha-methylstyrene by Fe₃O₄/tart-NPs, the remarkable enantioselectivity of 33% was obtained (entry 5). The L-tartaric acid as capping agent in Fe₃O₄/tart-NPs affects the enantioselectivity and sterogenic centre configuration of the epoxid (compare entries of 5 and 6). Although the mixture of (FeCl₃·6H₂O + L-tartaric acid) catalysed the oxidation of alpha-methylstyrene with 74% epoxide selectivity, its enantioselectivity was very low (5%) and the configuration of the epoxide was opposite to that obtained by Fe₃O₄/tart-NPs (entry 6). Catalyst Fe₃O₄/tart-NPs was also tested for the oxidation of cis- and trans-stilbene (entries 8 and 9). cis-

Stilbene is a frequently used substrate for the study of olefin epoxidation mechanism[51] because of mechanistic information associated with the ratio of cis- and trans-isomers in the stilbene oxide product. trans-Stilbene oxide was formed as the main product of the both oxidation, but epoxide selectivity for cis-stilbene was much higher (entries 8 and 9). This finding shows the important role of steric effect in determining the product selectivity by this catalyst. The side product of benzaldehyde was formed from the breaking of the olefin double bond which is comparable in the case of the trans-stilbene (44%). The oxidation reaction probably proceeds through a benzyl radical intermediate, which is sufficiently stable and allows free rotation about the C-C bond axis. The formation of trans-stilbene oxide from cis- and trans-stilbenes as the main product via a radical intermediate is expected due to the higher thermodynamic stability of the trans in comparison to the cis stereoisomer, in which the phenyl groups are located in anti-position with respect to each other. Interestingly, the catalyst was also found to be useful for the enantioselective sulfoxidation of thioanisole and hydroxylation of tetralin (entries 10 and 11). Thioanisol was oxidized to the sulfoxide in 100% selectivity, 36% conversion and 78% ee. This activity is close to the reported studies by H₂O₂. Bolm reported on the use of an asymmetric Schiff base/Fe(acac)₃/H₂O₂ which catalyzed the formation of sulfoxides in up to 90% ee, albeit in low moderate yields.[52] This was improved in later work through the use of a lithium carboxylate additive to the sulfoxide in 63% yield and 90% ee.[53] Immobilized manganese(II) complex, [{Mn(H₂O)₂Cl₂}₂(H₂Btar)], on mesoporous support SBA-15 (H₂L = 2,3-O-4-hydroxybenzhydrazidebenzylidene-D-tartrate) oxidaized thioanisole in 46% conversion, 29% sulfoxide selectivity and 100% ee.[54] Chiral sulfoxides are an important class of compounds as chiral auxiliaries in asymmetric carbon–carbon bond forming reactions,[55] as bioactive ingredients in the pharmaceutical industry[56] and constitute chiral synthons in organic synthesis for the preparation of biologically active compounds.[57] Tetralin was oxidized by O₂/isobutyraldehyde in the presence of Fe₃O₄/tart-NPs to 1-tetralol (22%) and 1-tetralone (3%) with 45% ee for 1-tetralol (entry 11). Tetralin is a convenient substance to choose for studying the autoxidation of the CH₂ group.[58] The intermediate radicals are, like the benzyl radical, resonance-stabilized systems on account of the presence in the molecule of the aromatic ring, which promotes exclusive attack at the alpha positions of tetralin in the reduced ring. Indene was not oxidized by Fe₃O₄/tart-NPs under the optimized condition and at 40 °C even after 24 h.
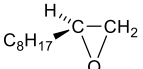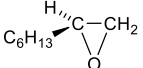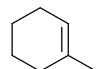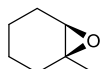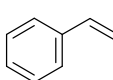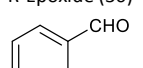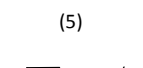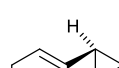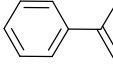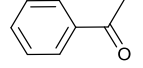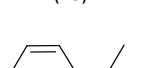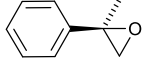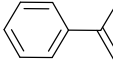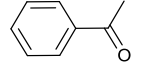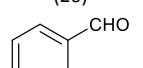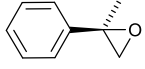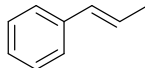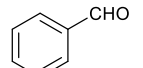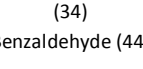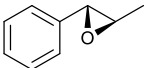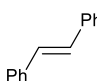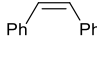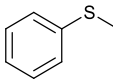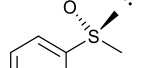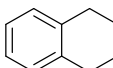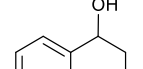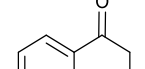
The catalytic activity and/or enantioselectivity of the present Fe₃O₄/tart-NPs are comparable and sometimes better than chiral Fe(III) complexes with complicated and difficult to synthesis ligands. Some comparisons are summarized in Table S1.

Journal Name

ARTICLE

Table 2 Asymmetric oxidation of olefins, thioanisole and tetralin by Fe_3O_4/tart-NPs [a]

Entry	Sub.	Conv. (%) [b]	Product(s) (Yield%) [b]			Epoxide Selectivity (%)	Ee (%) [c] (Config.)
1	1-Decene	77	R-Epoxide (77)			100	99 (R)
2	1-Octene[d]	48	R-Epoxide (48)			100	99 (R)
3		37	S-Epoxide (7)	R-Epoxide (30)		100	62 (R)
4 [d]		23	(5)	S-Epoxide (3)	R-Epoxide (15)	78	67 (R)
5		32	(20)	S-Epoxide (4)	R-Epoxide (8)	38	33 (R)
6 [e]		100	(26)	S-Epoxide (39)	R-Epoxide (35)	74	5 (S)
7 [d]		76	(34)	S-Epoxide (28)	R-Epoxide (14)	55	33 (S)
8 [f]		100 [g]	Benzaldehyde (44)	*trans*-Epoxide (48)	*cis*-Epoxide (8}	56	Nd [h]
9 [f]		100 [g]	Benzaldehyde (8)	*trans*-Epoxide (65)	*cis*-Epoxide (27)	92	Nd [h]
10		36%	R (33)	S (4)			78 (R)
11		25	S (16), R (6)	(3)			45 (S)

[a] Fe_3O_4/tart-NPs 1.0 mg, isobutyraldehyde 5 mmol, substrate 2 mmol, CH_3CN 3 ml, internal standard (chlorobanzene) 0.1 g, O_2 (2 bar), room temperature, time 7 h. [b] Conversion and yield were determined by GC and is an average of at least two runs. [c] The enantiomeric excess (*ee*) values were determined by GC analysis on a chiral stationary phase (see the Experimental section). [d] at 40 °C.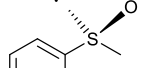 [e] Catalyst: $FeCl_3 \cdot 6H_2O$ 0.12 mmol + tart 0.02 mmol. [f] 0.5 mmol substrate. [g] Evaluated from ^1H NMR data. [h] Not determined

Journal Name

ARTICLE

Catalyst recycling

In order to investigate the possibility of several recycling runs for Fe$_3$O$_4$/tart-NPs, the solid catalyst was separated from the reaction mixture by an external magnet (Fig. 4). It was washed two times by acetonitrile and used again in a fresh reaction. The catalyst was recycled four times for cyclohexene oxidations (Fig. S4) and five times for tetralin oxidation (Fig. 5). FT-IR spectrum of the used and recovered Fe$_3$O$_4$/tart-NPs after first and fifth times are the same with that of the fresh one (Fig. S5). Therefore, recycling is possible in the case of Fe$_3$O$_4$/tart-NPs. As shown in Fig. 5, the increased activity of Fe$_3$O$_4$/tart-NPs is evident after each cycle. Enantiomeric excess (ee) increased in the first two recycles and then remained almost constant. Although, the particles size increases during the recycling process, the improvement of the catalyst efficiency after each use can be assigned to the well separation of Fe$_3$O$_4$/tart-NPs and reduction of the NPs aggregation which lead to higher surface area for the catalyst and its higher activity. This point is clearly seen in the SEM image of the used Fe$_3$O$_4$/tart nanoparticles (compare Fig. 3a and 3b). Reduction of the nanoparticles aggregation was also confirmed by an increase in the specific surface area of the catalyst Fe$_3$O$_4$/tart-NPs from 85 m^2 g^{-1} to 108 m^2 g^{-1} after two times recycle (Fig. S6). Increasing the particles size of the catalyst is partially due to the uncapping of the catalyst. Since presence of the tartaric acid is seen even after the 5th recycle of the catalysis (Fig. S5), separation of the capping ligand probably is occurred only to some extent. This conclusion was also confirmed by the occurrence of the enantioselective oxidation of tetralin. The homogeneous mixture of iron salt and L-tartaric acid shows very low enantioselectivity (Table 2, entry 6).
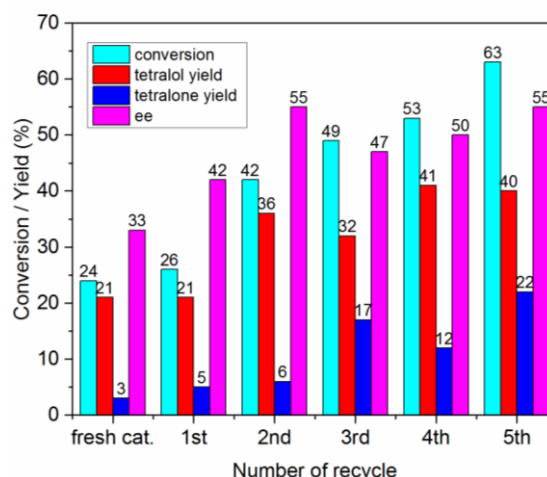
Fig. 5 Reuse of the catalyst in the aerobic oxidation of tetralin. Conditions: catalyst Fe$_3$O$_4$/tart-NPs 1.0 mg, isobutyraldehyde 5 mmol, substrate 2 mmol, CH$_3$CN 3 ml, chlorobanzene 0.1 g, oxygen 2 bar, time 7 h at 25 °C.

The possible oxidation mechanism

As a matter of fact, trace of the allyl ketone and 38% allyl alcohol were detected for the epoxidation of cyclohexene which is typically regarded as a good substrate to check for competition of olefin epoxidation vs. allylic oxidation (Table 1). This observation suggests that typical free radical intermediates are directly involved as potential oxidizing agents. Additional evidence for this was obtained from stereochemical investigations of the epoxidation of *cis*/*trans* stilbene (Table 2). Furthermore, electron-rich 1-methyl-1-cyclohexene with three substituent displayed a lower reactivity than cyclohexene with two electron donor substituent. This reflects the non-electrophilic nature of the oxygen transfer from the plausible intermediate to the olefin. The higher reactivity of cyclohexene relative to 1-methyl-1-cycohexene might be due to the greater steric effect around the double bond in the later. In the oxidation of *cis*- and *trans*-stilbene the steric effects were also distinct. The epoxide selectivity for the sterically demanding *trans*-stilbene was less than the *cis* isomer. On the other hand, the behaviour of *R*,*R*-tartaric (L-tartaric) acid adsorption on a Cu(110) surface using high-resolution surface analytical techniques has been studied.[24] Under certain conditions, the 2-dimensional order of the *R*,*R*-tartaric acid adlayer destroys all symmetry elements at the surface of Cu(111), leading to the creation of extended chiral surfaces. Such chiral surfaces may be an important factor in defining the active site in heterogeneous

Fig. 4 Separation of the dispersed catalyst Fe$_3$O$_4$/tart-NPs in acetonitrile (left) by using an external magnet (right).

enantioselective reactions. By considering all these information we may guess the probable mechanism for the aerobic enantioselective epoxidation by Fe_3O_4/tart-NPs.

The oxidation of cyclohexene with oxygen does not proceed without the presence of Fe_3O_4/tart-NPs nor without isobutyraldehyde (Table 1, entries 1, 5), which indicates that the chain reaction is initiated by interaction of isobutyraldehyde with Fe_3O_4/tart-NPs containing trivalent iron. The proposed mechanism is presented in Scheme 2, in which the conversions of an olefin and isobutyraldehyde observed in their co-oxidation in the presence of Fe_3O_4/tart-NPs are plotted. The initiation starts with the conversion of the aldehyde to the corresponding acyl radical (Scheme 2, A) catalysed by the nanocatalyst. Subsequently this radical reacts with O_2 producing an acylperoxy radical (Scheme 2, B) which is the intermediate, responsible for the transfer of oxygen from its molecular form in the gas phase to the products of olefin oxidation. This observation and the mechanism were similar to that of CuO@Ag nanowires[59] and cobalt-porphyrin/isobutyraldehyde/O_2 system[60] catalysts, which were used as the catalysts for stilbene oxidation.

The olefin coordinates to the Fe^{3+} of Fe_3O_4/tart-NPs surface (Scheme 2, C). The reaction then proceeds on the surface of magnetite nanoparticles by attacking of the acylperoxy radical on the coordinated olefin (Scheme 2, D), which results finally to the enantiomeric epoxide and isobutyric acid. The observed enantioselectivity can be rationalized by the nucleophlic coordination of the olefin to the Fe^{3+} of the Fe_3O_4/tart-NPs surface (Scheme 2, C). Although detailed considerations on the transition state are not yet clear, the stereochemistry of all the products indicates that Fe_3O_4/tart-NPs approaches the carbon-carbon double bond preferentially from the pro-S face of the olefin plane consisting of RCH=CHR' group. Chirality is induced by the chiral L-tartaric acid when the olefin is coordinated to the nanocatalyst surface. Product analyses of the various olefin epoxidation (Table 2) proves that the R-face of the prochiral olefin is mainly preferred for oxygenation, thereby the adsorption of olefin is through pro-S face, as shown in Fig. 6-(I) for 1-decene. Facial selectivity in the addition of the olefin to Fe_3O_4/tart would be established by hydrogen bond interaction between the hydrogen atom on the olefin double bond and the hydroxyl group of the tartrate (suggested transition state (III) in Fig. 6 for 1-decene). Similar intermediate has been proposed for the asymmetry achieved in the osmium tetroxide oxidation of olefins by employing chiral amines.[28,29]
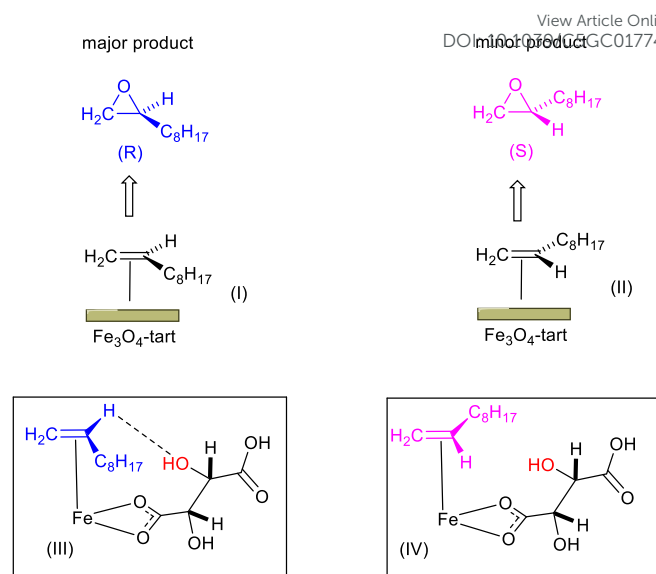
Fig. 6 The proposed intermediate for the adsorbed olefin (exemplified by 1-decene) on Fe_3O_4/tart-NPs

Coordination of the acylperoxy radical intermediate species to the transition metal–β-diketonate complexes has been reported by Nolte et al.[61] It was found that the metal catalyst (β-diketonate–transition metal complexes) is not only an efficient initiator of the reaction, but is also believed to enhance the reactivity of acylperoxy radical intermediate species in the oxidation process by allowing these to co-ordinate to the metal center. Even if the exact role of the metal catalyst in the epoxidation of olefins by dioxygen with co-oxidation of aldehydes is still unclear, studies by Valentine and coworkers[62] demonstrate that it coordinates to the acylperoxy radicals generated in the autooxidation of the aldehyde forming a metal-acylperoxo complex. That being so, iron(IV)–acylperoxo or iron(V)–oxo species derived by oxygen–oxygen bond cleavage of the acylperoxo group, probably play the role of active epoxidizing agents. High-valent Fe=O species are suggested as the actual active oxygen transfer agents in biological mono-oxygenations in both heme and non-heme iron enzymes and model systems.[63] However, rationalization of the Fe_3O_4/tart-NPs enantioselectivity by coordination of the acylperoxy radical to the Fe is difficult.

Journal Name

ARTICLE
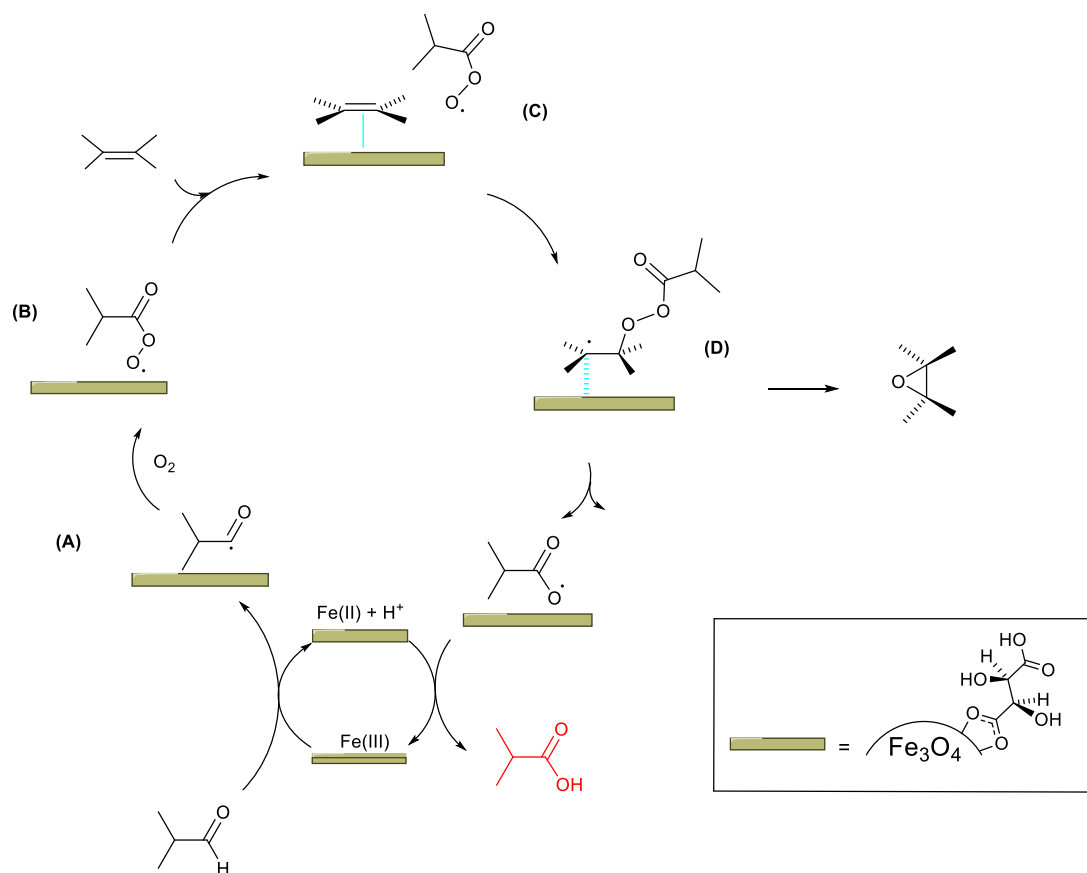
Scheme 2 The tentative mechanism for the oxidation of prochiral olefins by oxygen in the presence of Fe₃O₄/tart-NPs and isobutyraldehyde.

Conclusions

A chiral carboxylic acid stabilized magnetite nanoparticles have been shown to be an active, stable and good enantioselective catalyst for the production of asymmetric epoxide, sulfoxide and 1-tetralol using oxygen and isobutyraldehyde at room temperature. This oxidation system provides a general and ecofriendly method for the synthesis of chiral epoxides, which are one of the most valuable and versatile building blocks in the synthesis of chiral compounds. To the best of our knowledge, this is the first report on iron-catalyzed asymmetric aerobic oxidation by an inexpensive and easily prepared asymmetric magnetite nanoparticles and O₂, allowing for general epoxidation of a relatively wide variety of olefins in good yield and ee values up to greater than 99%. Moreover, the synthesized heterogeneous nanocatalysts possess strong magnetic responsivity due to a high saturation magnetization value (~60 emu g⁻¹). After completion of the reaction, the catalysts can be collected by simple magnetic decantation. In addition, the heterogeneous nanocatalysts are relatively stable and can be reused five times with increasing catalytic after each use in the catalytic process. Because of its simple recyclability, the catalyst is well-suited for continuous processes. Also, the method exhibits a number of highly favourable practical characteristics: (1) very good enantioselectivity in the oxidation of unfunctionalized olefins, thioaniol and tetralin, (2) oxygen can be used as the oxidant, (3) acetonitrile, a standard organic solvent which is not as harmful as halogenated compounds like CH₂Cl₂ or CHCl₃, is the reaction medium, (4) room temperature reaction and (5) all of the catalyst components (FeCl₃ salt, L-(+)-tartaric acid) are inexpensive, stable, and commercially available reagents.

COMMUNICATION

## References

1   V. Farina, J. T. Reeves, C. H. Senanayake and J. J. Song, *Chem. Rev.,* 2006, **106**, 2734.

2   F. G. Gelalcha, B. Bitterlich, G. Anilkumar, M. K. Tse and M. Beller, *Angew. Chem., Int. Ed.*, 2007, **46**, 7293.

3   H. C. Kolb, M. G. Finn and K. B. Sharpless, *Angew. Chem.*, 2001, **113**, 2056; *Angew. Chem. Int. Ed.*, 2001, **40**, 2004.

4   O. Lifchits, C. M. Reisinger and B. List, *J. Am. Chem. Soc.*, 2010, **132**, 10227; Y. Nishikawa and H. Yamamoto, *J. Am. Chem. Soc.,* 2011, **133**, 8432; H. Tanaka, H. Nishikawa, T. Uchida and T. Katsuki, *J. Am. Chem. Soc.,* 2010, **132**, 12034.

5   W. Dai, J. Li, G. Li, H. Yang, L. Wang and S. Gao, *Org. Lett.*, 2013, **15**, 4138.

6   S. Enthaler, K. Junge and M. Beller, *Angew. Chem., Int. Ed.,* 2008, **47**, 3317; K. Junge, K. Schröder and M. Beller, *Chem. Commun.*, 2011, **47**, 4849; G. Bauer and K. A. Kirchner, *Angew. Chem., Int. Ed.,* 2011, **50**, 5798; M. Darwish and M. Wills, *Catal. Sci. Technol.*, 2012, **2**, 243.

7   P. C. Bulman Page, A. Mace, D. Arquier, D. Bethell, B. R. Buckley, D. J. Willock and G. J. Hutchings, *Catal. Sci. Technol.,* 2013, **3**, 2330.

8   L. M. Rossi, N. J. S. Costa, F. P. Silva, R. Wojcieszak, *Green Chem.*, 2014, **16**, 2906; R. B. Nasir Baig and R. S. Varma, *Chem. Commun.,* 2012, **48**, 6220.

9   R. Mrówczyński, A. Nan and J. Liebscher, *RSC Adv.*, 2014, **4**, 5927.

10 V. Polshettiwar, R. Luque, A. Fihri, H. Zhu, M. Bouhrara and J. M. Basset, *Chem. Rev.*, 2011, **111**, 3036.

11 J. Sun, G. Yu, L. Liu, Z. Li, Q. Kan, Q. Huo and J. Guan, *Catal. Sci. Technol.*, 2014, **4**, 1246.

12 M. Ikenberry, L. Peña, D. Wei, H. Wang, S. H. Bossmann, T. Wilke, D. Wang, V. R. Komreddy, D. P. Rillema and K. L. Hohn, *Green Chem.*, 2014, **16**, 836.

13 A. Hu, S. Liu and W. Lin, *RSC Adv.*, 2012, **2**, 2576.

14 M. B. Gawande, P. S. Branco and R. S. Varma, *Chem. Soc. Rev.*, 2013, **42**, 3371.

15 Y. N. Zhao, B. Yu, Z. Z. Yang and L. N. He, *RSC Adv.*, 2014, **4**, 28941.

16 H. Egami and T. Katsuki, *J. Am. Chem. Soc.*, 2009, **131**, 6082.

17 V. Subramanian, D. W. Jeong, W. B. Han, W. J. Jang, J. O. Shim, J. W. Bae and H. S. Roh, *New J. Chem.*, 2014, **38**, 4872.

18 R. Cano, M. Yus and D. J. Ramón, *Chem. Commun.*, 2012, **48**, 7628.

19 M. Godoi, D. G. Liz, E. W. Ricardo, M. S.T. Rocha, J. B. Azeredo and A. L. Braga, *Tetrahedron*, 2014, **70**, 3349.

20 D. Zhang, C. Zhaou, Z. Sun, L. Wu, C. Tung and T. Zhang, *Nanoscale*, 2012, **4**, 6244.

21 H. Hosseini-Monfared, F. Parchegani and S. Alavi, *J. Colloid Interface Sci.*, 2015, **437**, 1.

22 O. Y. Lyakin, R. V. Ottenbacher, K. P. Bryliakov and E. P. Talsi, *ACS Catal.*, 2012, **2**, 1196.

23 O. Jacques, S. J. Richards and R. F. W. Jackson, *Chem. Commun.,* 2001, 2712.

24 M. Ortega Lorenzo, S. Haq, T. Bertrams, P. Murray, R. Raval and C. J. Baddeley, *J. Phys. Chem. B* 1999, **103***,* 10661.

25 J. -E. Bäckvall, Ed. *Modern Oxidation Methods*, Wiley-VCH, Weinheim, 2004.

26 B. S. Lane and K. Burgess, *Chem. Rev.*, 2003, **103**, 2457; M. Beller, *Adv. Synth. Catal.*, 2004, **346**, 107; G.-J. ten Brink, I. W. C. E. Arends and R. A. Sheldon, *Chem. Rev.*, 2004, **104**, 4105; R. Irie and T. Katsuki, *Chem. Records*, 2004, **4**, 96; Kaczorowaka, K.; Kolarska, Z.; Mitka, K.; Kowalski, P. *Tetrahedron*, 2005, **61**, 8315.

27 T. Mukaiyama and T. Yamada, *Bull. Chem. Soc. Jpn.*, 1995, **68**, 17; T. Takai, T. Yamada, S. Inoki, E. Hata and T. Mukaiyama, in *The Activation of Dioxygen and Homogeneous Catalytic Oxidation,*ed. D. H. R. Barton, Plenum Press, New York, 1993, p.133.

28 M. Tokles and J. K. Snyder, *Tetrahedron Lett.* 1986, **27**, 3951.

29 T. Yamada and K. Narasaka, *Chem. Lett.*, 1986, 131.

30 J. Govan and Y. K. Gun'ko, *Nanomaterials*, 2014, **4**, 222; .B. Nasir Baig, M. N. Nadagouda, R. S. Varma, *Coord. Chem. Rev.*, 2015, **287**, 137.

31 B. Dong, D. L. Miller and C. Y. Li, J. Phys. *Chem. Lett.*, 2012, **3**, 1346.

32 J. Zheng, Y. Dong, W. Wang, Y. Ma, J. Hu, X. Chen and X. Chen, *Nanoscale*, 2013, **5**, 4894.

33 M. F. Casula, Y.W. Jun, D. J. Zaziski, E. M. Chan, A. Corrias and A. P. Alivisatos, *J. Am. Chem. Soc.*, 2006, **128**, 1675.

34 D. L. A. de Faria, S. V. Silva and M. T. de Oliveira, *J. Raman Spectrosc.*, 1997, **28**, 873.

35 K. Moovendaran, V. Jayaramakrishnan and S. Natarajan, *Photonics and Optoelectronics*, 2014, **3,** 9.

36 K. Nakamoto, *Infrared and Raman Spectra of Inorganic and Coordination Compounds*, fourth ed., Wiley, New York, 1986. p 232.

37 W. Li, B. Zhang, X. Li, H. Zhang and Q. Zhang, *Appl. Catal., A*, 2013, **459**, 65.

38 J. Jia, J. C. Yu, X. -M. Zhu, K. M. Chan and Y. -X. J. Wang, *J. Colloid Interface Sci.*, 2012, **379**, 1; K. V. P. M. Shafi, A. Ulman, X. Z. Yan, N. Yang, C. Estournes, H. White and M. Rafailovich, *Langmuir*, 2001, **17**, 5093; Y. T. Tao, *J. Am. Chem. Soc.*, 1993, **115**, 4350; E. Karaoğlu, A. Baykal, M. Şenel, H. Sözeri and M. S. Toprak, *Mater. Res. Bull.*, 2012, **47**, 2480.

39 S. M. Barlow and R. Raval, *Surf. Sci. Rep.*, 2003, **50**, 201.

40 U. Schwertmann and R. Cornell, *Iron Oxides in the Laboratory - Preparation and Characterization*, Wiley-VCH, Weinheim, 2nd ed., 2000, pp. 5–28.

41 W. Cai and J.Q. Wan, *J. Colloid Interface Sci.*, 2007, **305**, 366.

42 T. Rajh, L. X. Chen, K. Lukas, T. Liu, M. C. Thurnauer and D. M. Tiede, *J. Phys. Chem. B*, 2002, **106**, 10543.

43 D. F. Evans and H. Wennerstrom, *The Colloidal Domain*, Wiley-VCH, New York, 2nd ed., 1999.

44 S. Sadighian, K. Rostamizadeh, H. Hosseini-Monfared and M. Hamidi, *Colloids Surf., B*, 2014, **117**, 406.

45 A. J. Appleton, S. Evans and J. R. Lindsay Smith, *J. Chem. Soc. Perkin Trans. 2*, 1996, 281.

46 G. B. Payne, P. H. Deming and P. H. Williams, *J. Org. Chem.*, 1961, **26**, 659.

47. V. Gutmann, *Coord. Chem. Rev.*, 1976, **18**, 225.

48 R. A. Sheldon, *A history of oxygen activation: 1773-1993*, in *The activation of dioxygen and homogeneous catalytic oxidation*, ed. D. H. Barton, A. E. Martell and D. T. Sawyer, Plenum Press, New York, 1993, p. 11.

49 T. Mukaiyama and T. Yamada, *Bull. Chem. Soc. Jpn.*, 1995, **68**, 17.

50 I. Tabushi and N. Koga, *J. Am. Chem. Soc.*, 1979, **101**, 6456.

51 W. Adam, K. J. Roschmann, C. R. Saha-Möller and D. Seebach, *J. Am. Chem. Soc.*, 2002, **124**, 5068.

52 J. Legros and C. Bolm, *Angew. Chem., Int. Ed.*, 2003, **42**, 5487.

53 J. Legros and C. Bolm, *Chem.–Eur. J.*, 2005, **11**, 1086.

54 S. Alavi, H. Hosseini-Monfared, P. Aleshkevych, *RSC Adv.*, 2014, **4**, 48827.

55 I. Fernandez and N. Khiar, *Chem. Rev.*, 2003, **103**, 3651.

56 H. Cotton, T. Elebring, M. Larsson, L. Li, H. Sorensen and S. von Unge, *Tetrahedron: Asymmetry*, 2000, **11**, 3819.

57 J. Legros, J. R. Dehli and C. Bolm, *Adv. Synth. Catal.*, 2005, **347**, 19.

58 H. Hock and W. Susemihl, *Ber.*, 1933. **66**, 61.

59 Z. Ye, L. Hu, J. Jiang, J. Tang, X. Cao and H. Gu, Catal. Sci. Technol., 2012, 2, 1146.

60 J. Haber, M. Kłosowski and J. Połtowicz, J. Mol. Catal. A: Chem., 2003, 201, 167.

61 B. B. Wentzel, P. A. Gosling, M. C. Feiters and R. J. M. Nolte, J. Chem. Soc., Dalton Trans., 1998, 2241.

62 W. Nam, H. J. Kim, S. H. Kim, R. Y. N. Ho and J. S. Valentine, Inorg. Chem., 1996, 35, 1045 and the references therein.

63 F. G. Gelalcha, G. Anilkumar, M. K. Tse, A. Brückner and M. Beller, Chem. Eur. J., 2008, 14, 7687 and the references therein.

Green Chemistry Accepted Manuscript
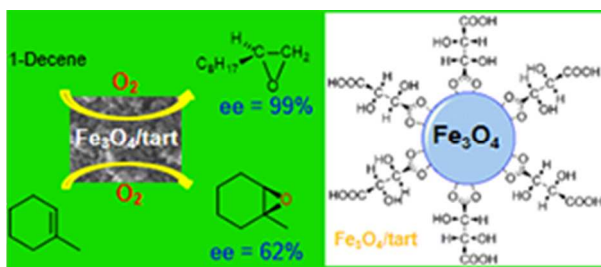
Magnetite nanoparticles stabilized by L-(+)-tartaric acid show high to excellent enantioselectivity in the aerobic epoxidation of olefins